

Elastic scattering of three ultracold bosons

P. M. A. Mestrom,* V. E. Colussi, T. Secker, and S. J. J. M. F. Kokkelmans
Eindhoven University of Technology, P. O. Box 513, 5600 MB Eindhoven, The Netherlands
(Dated: December 15, 2024)

Elastic scattering of three bosons at low energy is a fundamental problem in the many-body description of ultracold Bose gases, entering via the three-body scattering hypervolume D . We study this quantity for identical bosons that interact via a pairwise finite-range potential. Our calculations cover the regime from strongly repulsive potentials towards attractive potentials supporting multiple two-body bound states and are consistent with the few existing predictions for D . We present the first numerical confirmation of the universal predictions for D that are made in the strongly-interacting regime, where Efimov physics dominates, for a local nonzero-range potential. Our findings highlight how finite-range effects, such as d -wave interactions, become important as the interaction strength is reduced.

PACS numbers: 31.15.-p, 34.50.-s, 67.85.-d

Introduction.—Due to the precise experimental control of interatomic interactions via external magnetic fields, ultracold atomic gases have emerged as a versatile field for studying and manipulating quantum systems. The effective two-body interaction strength given by the s -wave scattering length a can be tuned via Feshbach resonances [1]. When $|a|$ diverges, Efimov predicted the existence of an infinite number of three-body bound states whose universal scaling properties have been observed experimentally [2–8]. This non-perturbative three-body effect influences the bulk properties of strongly-interacting Bose gases [9–13] and Bose-Einstein condensates (BECs) interacting with an impurity particle [14–17]. Connecting few-body processes with bulk properties of ultracold Bose gases is fundamental to our understanding of these quantum many-body systems.

This connection is evident from a low-density expansion of the ground-state energy density of a dilute BEC with a homogeneous number density n [18]:

$$\mathcal{E} = \frac{2\pi\hbar^2 n^2 a}{m} \left\{ 1 + \frac{128}{15\sqrt{\pi}} \sqrt{na^3} + \left[\frac{8(4\pi-3\sqrt{3})}{3} \ln(na^3) + \frac{D}{12\pi a^4} + \pi r_s/a + 118.5 \right] na^3 + \dots \right\} \quad (1)$$

where the dots indicate higher-order correction terms in the diluteness parameter na^3 , m is the mass of a boson, r_s is the two-body effective range, and $a > 0$. The $\sqrt{na^3}$ correction, calculated by Lee, Huang and Yang (LHY) [19, 20], originates from two-body elastic scattering characterized by a alone. Experiments have probed LHY physics by measuring the critical temperature of a BEC [21], quantum depletion [22], excitation spectrum [23, 24], thermodynamic equation of state [25] and contact [26]. Additionally, recent studies predicted [27] and experimentally confirmed the formation of quantum

droplets in mixtures [28–30] and dipolar BECs [31–33] due to a stabilizing force originating from the LHY correction.

As the study of strongly-interacting Bose gases advances, there is the opportunity to observe beyond-LHY corrections. Elastic three-body scattering determines the first beyond-LHY corrections given by the $\ln(na^3)$ correction calculated by Wu [34–36] and the *hypervolume* D which is defined by the three-body scattering wave function at zero collision energy [18]. D determines the effective three-body interaction similar to a in the two-body case [18], is predicted to act as a stabilizing force for quantum droplets in ultracold Bose gases [37–39], and may be tuned experimentally [40]. Previous works have included three-body effects via phenomenological extensions of the Gross-Pitaevskii equation [37–39, 41–46]. The first beyond LHY-corrections have been studied from a microscopic theory using quantum Monte Carlo simulations [47, 48] and by studying three-body elastic scattering of ultracold bosons in vacuum [18, 49–51].

Despite its fundamental relevance, low-energy elastic three-body scattering remains sparsely explored. This is partly caused by the difficulty to isolate scattering events from the elastic three-body scattering amplitude to obtain the hypervolume D [4, 6, 49, 52]. The imaginary part of D is proportional to the three-body recombination rate [4, 53] which has been studied extensively for various three-body systems, both experimentally and theoretically [54]. Universal behavior has been predicted for the strongly-interacting regime where Efimov physics plays a dominant role leading to a log-periodic behavior of D [4, 6, 51, 55]. For short-range pairwise potentials, D has been studied considering the repulsive hard-sphere potential [18] and a Gaussian interaction potential [53]. However, the behavior of D over a full range of interaction strengths has not been explored for any finite-range potential, which demonstrates the highly nontrivial character of this problem.

In this Letter, we investigate the three-body scattering hypervolume D for identical bosons interacting via a pairwise square-well potential, covering the range

*Corresponding author: p.m.a.mestrom@tue.nl

from weak to strong interactions, and analyze the corresponding universal and nonuniversal effects. We present the first numerical calculations of D in the strongly-interacting regime involving a local finite-range potential, and study the corresponding Efimov universality. Besides the Efimov resonances, we identify additional three-body resonances close to two-body d -wave resonances and study their character.

Elastic three-body scattering amplitude.—A convenient way to calculate D is to use the Faddeev equations for the three-particle transition operators $U_{\alpha\beta}$ in the form presented by Alt, Grassberger and Sandhas (AGS) [56, 57],

$$\begin{cases} U_{00}(z) = \sum_{\alpha=1}^3 T_{\alpha}(z)G_0(z)U_{\alpha 0}(z) \\ U_{\alpha 0}(z) = G_0^{-1}(z) + \sum_{\substack{\beta=1 \\ \beta \neq \alpha}}^3 T_{\beta}(z)G_0(z)U_{\beta 0}(z) \end{cases} \quad (2)$$

for $\alpha = 1, 2, 3$,

to find the transition amplitude for three-body elastic scattering that is described by the operator $U_{00}(z)$. Here z is the (complex) three-body energy. The index α (β) in $U_{\alpha\beta}(z)$ labels the four possible configurations for the outgoing (incoming) state of the three-body scattering wave

function, i.e., $\alpha = 0$ denotes three free particles, whereas $\alpha = 1, 2$ and 3 stand for the three possible atom-dimer configurations. $T_{\alpha}(z)$ represents the transition operator for scattering between particles β and γ ($\beta, \gamma = 1, 2, 3$, $\beta \neq \gamma \neq \alpha$) in the presence of particle α and is simply related to the two-body T -operator $T(z_{2b})$ [58], where z_{2b} is some complex value for the energy of the two-body system. The operator $G_0(z)$ is the free three-body Green's function $(z - H_0)^{-1}$ where H_0 is three-body kinetic energy operator in the center-of-mass frame of the three-particle system.

The three-body configuration is parametrized by the Jacobi momenta $\mathbf{p}_{\alpha} = (\mathbf{P}_{\beta} - \mathbf{P}_{\gamma})/2$ and $\mathbf{q}_{\alpha} = (2/3)(\mathbf{P}_{\alpha} - (\mathbf{P}_{\beta} + \mathbf{P}_{\gamma})/2)$ where \mathbf{P}_{α} represents the momentum of particle α in the three-body center-of-mass frame. There exist three possibilities to choose these Jacobi vectors. If we define $\mathbf{q} \equiv \mathbf{q}_1$ and $\mathbf{p} \equiv \mathbf{p}_1$, we have $\mathbf{q}_2 = \mathbf{p} - \mathbf{q}/2$, $\mathbf{p}_2 = -\mathbf{p}/2 - 3\mathbf{q}/4$, $\mathbf{q}_3 = -\mathbf{p} - \mathbf{q}/2$ and $\mathbf{p}_3 = -\mathbf{p}/2 + 3\mathbf{q}/4$. This parametrization is suitable for relating the matrix element $\langle \mathbf{p}, \mathbf{q} | U_{00}(0) | \mathbf{0}, \mathbf{0} \rangle$ to the hypervolume D where we normalize the plane wave states according to $\langle \mathbf{p}' | \mathbf{p} \rangle = \delta(\mathbf{p}' - \mathbf{p})$. From Tan's definition of the three-body scattering hypervolume D [18], we deduce the following relation between $\langle \mathbf{p}, \mathbf{q} | U_{00}(0) | \mathbf{0}, \mathbf{0} \rangle$ and D (see supplemental material [59]):

$$\begin{aligned} \langle \mathbf{p}, \mathbf{q} | U_{00}(0) | \mathbf{0}, \mathbf{0} \rangle = \sum_{\alpha=1}^3 \left\{ \delta(\mathbf{q}_{\alpha}) \langle \mathbf{p}_{\alpha} | T(0) | \mathbf{0} \rangle - \frac{1}{2\pi^4} \frac{a^2}{m\hbar^2} \frac{1}{q_{\alpha}^2} + \frac{1}{12\pi^4} (4\pi - 3\sqrt{3}) \frac{a^3}{m\hbar^3} \frac{1}{q_{\alpha}} + \frac{1}{3\pi^5} (4\pi - 3\sqrt{3}) \frac{a^4}{m\hbar^4} \ln\left(\frac{q_{\alpha}|a|}{\hbar}\right) \right. \\ \left. - \frac{p_{\alpha}^2 + \frac{3}{4}q_{\alpha}^2}{q_{\alpha}^2} m \langle \mathbf{0} | T(0) | \mathbf{0} \rangle \frac{\partial^2 \langle \mathbf{p} | T(0) | \mathbf{0} \rangle}{\partial p^2} \right\}_{p=0} + \frac{1}{3} \frac{1}{(2\pi)^6} \frac{D}{m\hbar^4} + \mathcal{O}\left(q_{\alpha} \ln\left(\frac{q_{\alpha}|a|}{\hbar}\right), \frac{p_{\alpha}^2}{q_{\alpha}}\right) \end{aligned} \quad (3)$$

which holds for any local symmetric two-body potential.

We consider three identical bosons that interact via a pairwise square-well potential

$$V(r) = \begin{cases} -V_0, & 0 \leq r < R, \\ 0, & r \geq R, \end{cases} \quad (4)$$

where r denotes the relative distance between two particles. We solve the AGS equations given in Eq. (2) for the matrix element $\langle \mathbf{p}, \mathbf{q} | U_{00}(0) | \mathbf{0}, \mathbf{0} \rangle$ [59]. The dimension of this set of integral equations is reduced to one by expanding this amplitude in spherical harmonics and in two-body states that are determined by the Weinberg expansion and are thus related to two-body bound states or resonances [58, 60]. The resulting integral equation is solved as a matrix equation by discretizing the momenta. The three-body scattering hypervolume is obtained from Eq. (3). Our method differs from another approach recently presented by Zhu and Tan [53] who calculated the hypervolume D from the zero-energy three-body scatter-

ing wave function in position space for a variable two-body Gaussian potential. Their method is limited by their numerics to the weakly-interacting regime in contrast to our approach. We have calculated the three-body scattering hypervolume D in the complete regime ranging from strongly repulsive potentials, i.e., $V_0 \rightarrow -\infty$, towards attractive potentials supporting multiple two-body bound states as shown in Fig. 1, and we have explored both the weakly- and strongly-interacting regime, i.e., $a/R \lesssim 1$ and $a/R \gg 1$, respectively, by tuning the potential depth V_0 .

Repulsive potentials.—In the limit $V_0 \rightarrow -\infty$, the square-well potential approaches the hard-sphere (HS) interaction that was considered already a decade ago by Tan [18]. The upper right inset of Fig. 1 shows that the three-body scattering hypervolume approaches the hard-sphere limit within the numerical accuracy of our approach:

$$D_{HS}/a^4 = 1761 \pm 1. \quad (5)$$

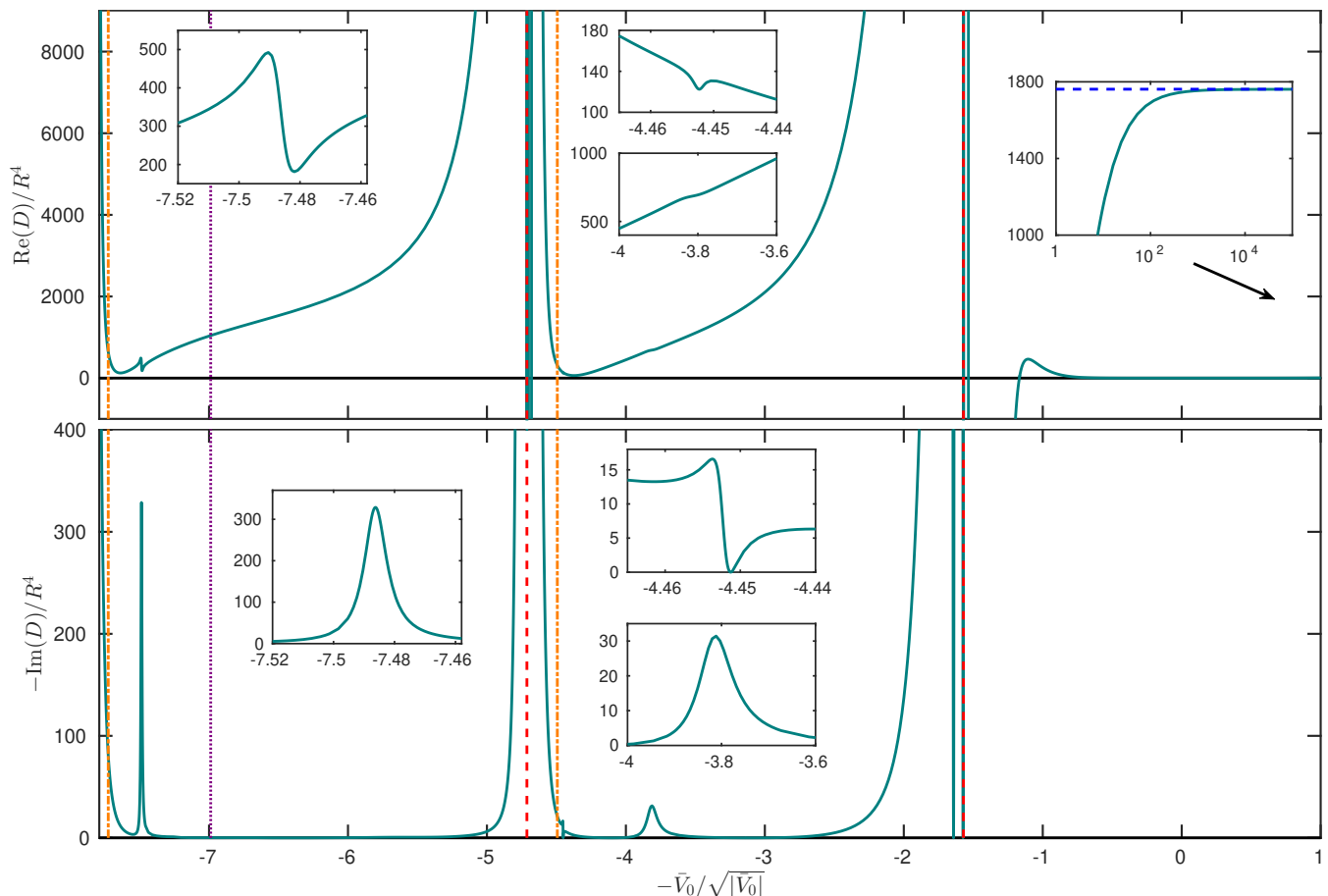


Figure 1: Three-body scattering hypervolume D corresponding to the square-well potential as a function of the dimensionless interaction strength $\bar{V}_0 = mV_0R^2/\hbar^2$. The vertical lines indicate the interaction strengths at which two-body states become bound: s -wave states ($l = 0$, red dashed lines) at $\bar{V}_0 = (\pi/2)^2$ and $(3\pi/2)^2$, d -wave states ($l = 2$, orange dash-dotted lines) at $\bar{V}_0 \approx (4.49341)^2$ and $(7.72525)^2$ and g -wave state ($l = 4$, purple dotted line) at $\bar{V}_0 \approx (6.98793)^2$. The inset on the right displays the behavior of D for strongly repulsive potentials as indicated by the black arrow. The horizontal blue dashed line represents the hard-sphere limit calculated by Ref. [18]. The other insets zoom in on the real and imaginary part of D near three resonances that arise from three-body quasibound states at the three-particle threshold.

When the potential barrier $-V_0$ is decreased, the hypervolume decreases as well, and it eventually goes to zero in the limit $|V_0| \rightarrow 0$ as

$$\begin{aligned}
 D &= -96\pi^6 m^2 \hbar^4 \langle \mathbf{0} | V | \mathbf{0} \rangle \frac{\partial^2 \langle \mathbf{p} | V | \mathbf{0} \rangle}{\partial p^2} \Big|_{p=0} + \mathcal{O}(\bar{V}_0^3) \\
 &= \frac{8}{15} \pi^2 \bar{V}_0^2 R^4 + \mathcal{O}(\bar{V}_0^3),
 \end{aligned} \tag{6}$$

where $\bar{V}_0 = mV_0R^2/\hbar^2$ denotes the dimensionless interaction strength. The bottom result in Eq. (6) applies specifically to the square-well potential, whereas the top result is a general relation for D for local symmetric potentials V in the zero-depth limit. For this general case, \bar{V}_0 is defined to be a prefactor of the potential as $V(r) = \bar{V}_0 f(r)$ where $f(r)$ is independent of \bar{V}_0 . We have analytically derived Eq. (6) from the AGS equations (see supplemental material [59]), and we have numerically confirmed it for the square-well potential. The general expression in

Eq. (6) is also consistent with the result derived by Zhu and Tan for a Gaussian potential (Eq. (10) of Ref. [53]).

Attractive potentials.—As the potential depth increases, two-body states start to become bound resulting in a nonzero value for the imaginary part of D . Fig. 1 shows that this value is much smaller than the magnitude of the real part in most regimes. Close to the potential resonances that are indicated by the vertical red dashed lines in Fig. 1, the hypervolume D scales as a^4 and its behavior becomes log-periodic due to the Efimov effect as we will see below. Besides the Efimov trimers in the strongly-interacting regime, additional three-body quasibound states might appear at the zero-energy threshold in the weakly-interacting regime. We identify several three-body resonances related to such trimer states at $\bar{V}_0 = 3.8, 4.45$ and 7.49 as indicated by the insets in Fig. 1. The presence of these three resonances depends critically on the inclusion of one term in our Weinberg expansion of the two-body T -operator, namely the one cor-

responding to the almost bound two-body d -wave state (vertical orange dash-dotted lines). Therefore we conclude that these three trimer states are associated with d -wave dimer states in a similar way as the universal three-body state for van der Waals potentials studied by Ref. [61]. Even though the three trimer resonances in the weakly-interacting regime have the same origin, the behavior of the real and imaginary part is not the same for all resonances. This suggests that the behavior of the hypervolume in the weakly-interacting regime depends on some three-body background phase shift resulting from the nonresonant pathways for elastic three-body scattering or three-body recombination [6].

Our results presented in Fig. 1 can be compared to the calculations of Zhu and Tan [53] for the hypervolume corresponding to a Gaussian two-body potential. Even though both results are very similar for repulsive potentials, they are quite different for attractive interactions. The main difference is the behavior of D when approaching the s -wave dimer resonances (vertical red dashed lines), where Ref. [53] finds additional trimer resonances that are different from the Efimov resonances. It is unclear where this difference comes from. However, the validity of the method presented in Ref. [53] breaks down when $|a|/R \gg 1$, which makes the comparison in that regime questionable. Secondly, we find that D behaves smoothly across the d -wave dimer resonances (vertical orange dash-dotted lines) in contrast to the results of Ref. [53]. This difference suggest that the behavior of D across a d -wave dimer resonance depends on the details of the considered two-body potential.

In the strongly-interacting regime ($|a|/R \gg 1$), the real part of the hypervolume D is expected to behave as

$$\text{Re}(D/a^4) \approx C \left(c_- + \frac{\frac{1}{2}b_- \sin(2s_0 \ln(a/a_-))}{\sin^2(s_0 \ln(a/a_-)) + \sinh^2(\eta)} \right) \quad (7)$$

for $a < 0$ and

$$\text{Re}(D/a^4) \approx C \left(c_+ + \frac{1}{2}b_+(1 - e^{-2\eta}) + b_+ e^{-2\eta} \sin^2(s_0 \ln(a/a_+) - \pi/4) \right) \quad (8)$$

for $a > 0$. Here $s_0 \approx 1.00624$ is the parameter that sets the periodicity in Efimov physics for identical bosons [2, 3] and we have defined the constant $C \equiv 64\pi(4\pi - 3\sqrt{3})$. The general form of Eq. (7) for $\eta = 0$ was first derived by Efimov [55], whereas Braaten et al. [51] first obtained the general form of Eq. (8) for $\eta = 0$. D’Incao [6] generalized both results by including the inelasticity parameter η that describes the tendency to decay to deeply bound dimer states. The parameters a_- and a_+ are known as the three-body parameters that locate the three-body recombination maxima and minima, respectively, and are completely determined by the interaction between the three particles [4]. The coefficients b_{\pm} and

c_{\pm} are universal in the sense that they do not depend on the short-range form of the potentials [6].

The imaginary part of D is proportional to the three-body recombination rate [4, 53]. The corresponding universal expressions in the strongly-interacting regime including the loss parameter η [4, 6, 62] are given by

$$\text{Im}(D/a^4) \approx -\frac{1}{2}C_- \frac{\sinh(2\eta)}{\sin^2(s_0 \ln(a/a_-)) + \sinh^2(\eta)} \quad (9)$$

for $a < 0$ and

$$\text{Im}(D/a^4) \approx -\frac{1}{2}C_+ \left(\frac{1}{4}(1 - e^{-4\eta}) + e^{-2\eta} \left(\sin^2(s_0 \ln(a/a_+)) + \sinh^2(\eta) \right) \right) \quad (10)$$

for $a > 0$. The constants C_{\pm} have been determined by previous studies and are given by $C_- \approx 4590$ [62] and $C_+ \approx 67.1177$ [63–65].

The universal relations (7) and (8) have not been numerically confirmed for any local nonzero-range two-body potential. We present the first of such calculations in Fig. 2 that covers the universal regime near the second potential resonance of the square-well potential, i.e., $\sqrt{V_0}$ is close to $3\pi/2$. Similar results for the first potential resonance can be found in the supplemental material [59]. The dashed curves display the analytic zero-range results given by Eqs. (7), (8), (9) and (10). In the supplemental material [59] we have determined the universal coefficients C_+ , b_{\pm} and c_{\pm} by analyzing the three-body scattering hypervolume for a contact interaction with a cut-off in momentum space, which resulted in $C_+ = 67.118(5)$, $b_+ = 0.0226(5)$, $c_+ = 1.1288(5)$, $b_- = 3.153(5)$ and $c_+ = 1.140(2)$. Our value for C_+ is in excellent agreement with the analytical prediction [63–65]. The values for the nonuniversal parameters a_{\pm} and η are given in the supplemental material [59] as well and are consistent with the results stated in Ref. [58].

Our results for the coefficients b_{\pm} and c_{\pm} can be compared to the values presented by Braaten et al. [51] who performed three-body calculations for a zero-range interaction. According to Ref. [51] the universal coefficients in Eqs. (7) and (8) are $b_- = 3.16$, $c_- = 1.14$, $b_+ = 0.021$ and $c_+ = 1.13$ (see supplemental material [59]). Our values for c_{\pm} and b_- agree with the results of Ref. [51]. Even though our value of b_+ deviates approximately 7% from the value of Ref. [51], it is only a deviation of 0.1% from the overall result for D (see Fig. S5 of the supplemental material [59]).

Conclusion.—By solving the AGS equations for the three-body elastic scattering amplitude, we have studied the behavior of the three-body scattering hypervolume D which is a fundamental quantity of ultracold three-body collisions and is needed for studying ultracold Bose gases beyond the LHY correction. We have presented the first numerical calculations of D for identical bosons

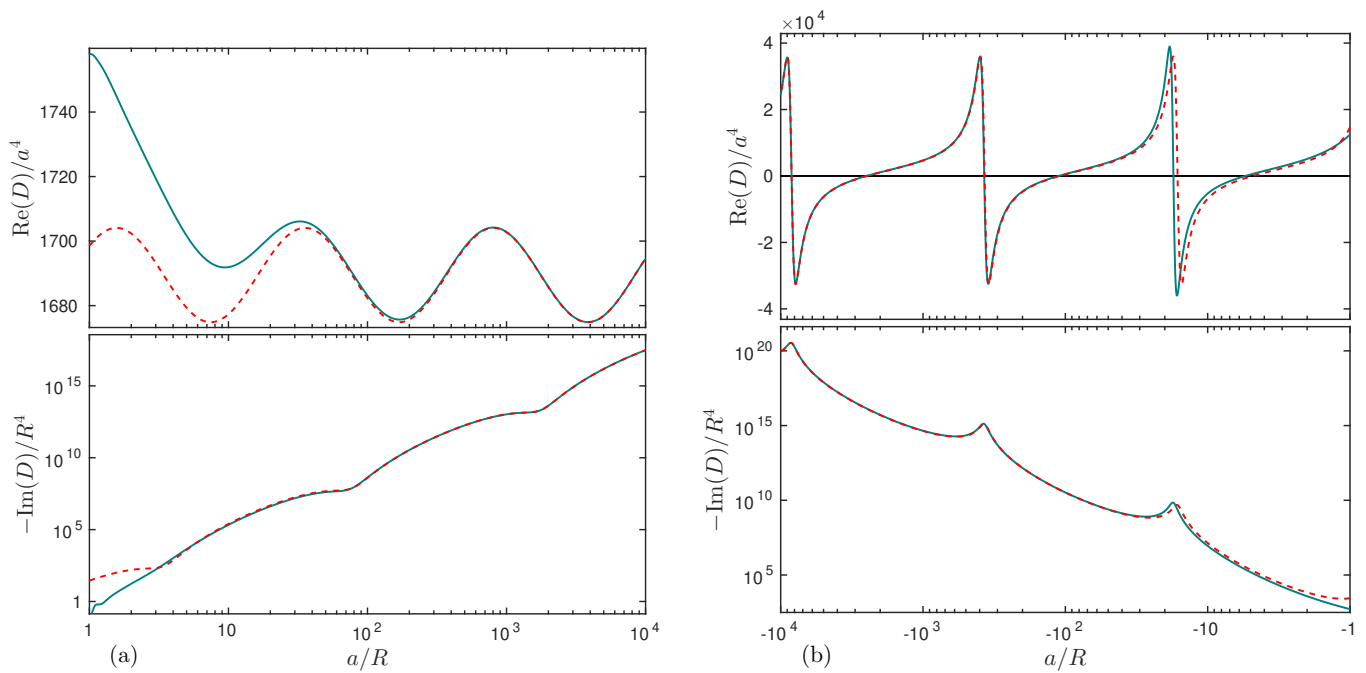


Figure 2: Three-body scattering hypervolume D near the second potential resonance of the square-well potential for (a) $a > 0$ and (b) $a < 0$. The dashed curves give the analytic zero-range results given by Eqs. (7), (8), (9) and (10) where we set $a_+/R = 1759$, $b_+ = 0.0226$, $c_+ = 1.1288$, $C_+ = 67.118$, $a_-/R = -8396$, $b_- = 3.153$, $c_- = 1.140$, $C_- = 4590$ and $\eta = 0.068$.

with a variable nonzero-range potential in the strongly-interacting regime. Our results agree with the universal predictions of Refs. [6, 51, 55] and show how finite-range effects start to play a role as the absolute value of the scattering length is decreased. For repulsive interactions, we have confirmed the hard-sphere limit from [18]. We have also explored the weakly-interacting regime for which no general theoretical predictions have been made. We have identified several three-body resonances related to trimer states that are associated with a d -wave dimer state, and we have derived a general formula for D that is valid as the potential depth or height goes to zero.

The approach outlined in this Letter is very general and can be applied to other types of two-body potentials as well. It would be particularly interesting to investigate the three-body hypervolume for van der Waals potentials to make quantitative predictions for ultracold atomic Bose gases. Our method could also be applied to mixtures, for which low-energy elastic three-body scattering

is completely unexplored to our knowledge. Additionally, one could extend our approach to study three-body elastic scattering embedded in a many-body environment in the spirit of Ref. [9] and determine how three-body correlations affect both stationary and dynamical observables of ultracold Bose gases for any short-range two-body potential. In particular, one could make quantitative predictions for the ground-state energy density of a BEC and investigate stabilizing effects from the three-body hypervolume for small negative scattering lengths including the formation of quantum droplets [37–39].

Acknowledgements.—We thank José P. D’Incao, Chris H. Greene, Silvia Musolino, Denise Braun and Gijs Groeneveld for useful discussions. This research is financially supported by the Netherlands Organisation for Scientific Research (NWO) under Grant 680-47-623, and is part of the research programme of the Foundation for Fundamental Research on Matter (FOM).

[1] C. Chin, R. Grimm, P. Julienne, and E. Tiesinga, *Rev. Mod. Phys.* **82**, 1225 (2010).
 [2] V. Efimov, *Phys. Lett. B* **33**, 563 (1970).
 [3] V. Efimov, *Yad. Fiz.* **12**, 1080 (1970), [*Sov. J. Nucl. Phys.* **12**, 589 (1971)].
 [4] E. Braaten and H.-W. Hammer, *Phys. Rep.* **428**, 259 (2006).
 [5] P. Naidon and S. Endo, *Rep. Prog. Phys.* **80**, 056001

(2017).
 [6] J. P. D’Incao, *Journal of Physics B: Atomic, Molecular and Optical Physics* **51**, 043001 (2018).
 [7] T. Kraemer, M. Mark, P. Waldburger, J. Danzl, C. Chin, B. Engeser, A. Lange, K. Pilch, A. Jaakkola, H.-C. Nägerl, et al., *Nature* **440**, 315 (2006).
 [8] B. Huang, L. A. Sidorenkov, R. Grimm, J. M. Hutson, et al., *Physical Review Letters* **112**, 190401 (2014).

- [9] V. E. Colussi, S. Musolino, and S. J. J. M. F. Kokkelmans, *Phys. Rev. A* **98**, 051601(R) (2018).
- [10] E. Braaten, D. Kang, and L. Platter, *Phys. Rev. Lett.* **106**, 153005 (2011).
- [11] F. Werner and Y. Castin, *Phys. Rev. A* **86**, 053633 (2012).
- [12] V. E. Colussi, J. P. Corson, and J. P. D’Incao, *Phys. Rev. Lett.* **120**, 100401 (2018).
- [13] V. E. Colussi, B. E. van Zwol, J. P. D’Incao, and S. J. J. M. F. Kokkelmans, arXiv:1901.10355v2 [cond-mat.quant-gas] (2019).
- [14] J. Levinsen, M. M. Parish, and G. M. Bruun, *Phys. Rev. Lett.* **115**, 125302 (2015).
- [15] S. M. Yoshida, S. Endo, J. Levinsen, and M. M. Parish, *Phys. Rev. X* **8**, 011024 (2018).
- [16] M. Sun, H. Zhai, and X. Cui, *Phys. Rev. Lett.* **119**, 013401 (2017).
- [17] P. Naidon, *Journal of the Physical Society of Japan* **87**, 043002 (2018).
- [18] S. Tan, *Phys. Rev. A* **78**, 013636 (2008).
- [19] T. D. Lee and C. N. Yang, *Phys. Rev.* **105**, 1119 (1957).
- [20] T. D. Lee, K. Huang, and C. N. Yang, *Phys. Rev.* **106**, 1135 (1957).
- [21] R. P. Smith, R. L. D. Campbell, N. Tammuz, and Z. Hadzibabic, *Phys. Rev. Lett.* **106**, 250403 (2011).
- [22] R. Lopes, C. Eigen, N. Navon, D. Clément, R. P. Smith, and Z. Hadzibabic, *Phys. Rev. Lett.* **119**, 190404 (2017).
- [23] S. B. Papp, J. M. Pino, R. J. Wild, S. Ronen, C. E. Wieman, D. S. Jin, and E. A. Cornell, *Phys. Rev. Lett.* **101**, 135301 (2008).
- [24] R. Lopes, C. Eigen, A. Barker, K. G. H. Viebahn, M. Robert-de Saint-Vincent, N. Navon, Z. Hadzibabic, and R. P. Smith, *Phys. Rev. Lett.* **118**, 210401 (2017).
- [25] N. Navon, S. Piatecki, K. Günter, B. Rem, T. C. Nguyen, F. Chevy, W. Krauth, and C. Salomon, *Phys. Rev. Lett.* **107**, 135301 (2011).
- [26] R. J. Wild, P. Makotyn, J. M. Pino, E. A. Cornell, and D. S. Jin, *Phys. Rev. Lett.* **108**, 145305 (2012).
- [27] D. S. Petrov, *Phys. Rev. Lett.* **115**, 155302 (2015).
- [28] C. R. Cabrera, L. Tanzi, J. Sanz, B. Naylor, P. Thomas, and L. Cheiney, *Science* **359**, 301 (2018).
- [29] P. Cheiney, C. R. Cabrera, J. Sanz, B. Naylor, L. Tanzi, and L. Tarruell, *Phys. Rev. Lett.* **120**, 135301 (2018).
- [30] G. Semeghini, G. Ferioli, L. Masi, C. Mazzinghi, L. Wolswijk, F. Minardi, M. Modugno, G. Modugno, M. Inguscio, and M. Fattori, *Phys. Rev. Lett.* **120**, 235301 (2018).
- [31] H. Kadau, M. Schmitt, M. Wenzel, C. Wink, T. Maier, I. Ferrier-Barbut, and T. Pfau, *Nature* **530**, 194 (2016).
- [32] I. Ferrier-Barbut, H. Kadau, M. Schmitt, M. Wenzel, and T. Pfau, *Phys. Rev. Lett.* **116**, 215301 (2016).
- [33] L. Chomaz, S. Baier, D. Petter, M. J. Mark, F. Wächtler, L. Santos, and F. Ferlaino, *Phys. Rev. X* **6**, 041039 (2016).
- [34] T. T. Wu, *Phys. Rev.* **115**, 1390 (1959).
- [35] K. Sawada, *Phys. Rev.* **116**, 1344 (1959).
- [36] N. M. Hugenholtz and D. Pines, *Phys. Rev.* **116**, 489 (1959).
- [37] A. Bulgac, *Phys. Rev. Lett.* **89**, 050402 (2002).
- [38] P. F. Bedaque, A. Bulgac, and G. Rupak, *Phys. Rev. A* **68**, 033606 (2003).
- [39] P. B. Blakie, *Phys. Rev. A* **93**, 033644 (2016).
- [40] D. S. Petrov, *Phys. Rev. Lett.* **112**, 103201 (2014).
- [41] N. Akhmediev, M. P. Das, and A. V. Vagov, *International Journal of Modern Physics B* **13**, 625 (1999).
- [42] A. Gammal, T. Frederico, L. Tomio, and P. Chomaz, *Journal of Physics B: Atomic, Molecular and Optical Physics* **33**, 4053 (2000).
- [43] A. Gammal, T. Frederico, L. Tomio, and P. Chomaz, *Phys. Rev. A* **61**, 051602(R) (2000).
- [44] S. K. Adhikari, *Phys. Rev. A* **66**, 013611 (2002).
- [45] H. Al-Jibbouri, I. Vidanović, A. Balaž, and A. Pelster, *Journal of Physics B: Atomic, Molecular and Optical Physics* **46**, 065303 (2013).
- [46] K.-T. Xi and H. Saito, *Phys. Rev. A* **93**, 011604(R) (2016).
- [47] S. Giorgini, J. Boronat, and J. Casulleras, *Phys. Rev. A* **60**, 5129 (1999).
- [48] M. Rossi, L. Salasnich, F. Ancilotto, and F. Toigo, *Phys. Rev. A* **89**, 041602(R) (2014).
- [49] Braaten, E. and Nieto, A., *Eur. Phys. J. B* **11**, 143 (1999).
- [50] T. Köhler, *Phys. Rev. Lett.* **89**, 210404 (2002).
- [51] E. Braaten, H.-W. Hammer, and T. Mehen, *Phys. Rev. Lett.* **88**, 040401 (2002).
- [52] R. D. Amado and M. H. Rubin, *Phys. Rev. Lett.* **25**, 194 (1970).
- [53] S. Zhu and S. Tan, arXiv:1710.04147v1 [cond-mat.quant-gas] (2017).
- [54] C. H. Greene, P. Giannakeas, and J. Pérez-Ríos, *Rev. Mod. Phys.* **89**, 035006 (2017).
- [55] V. Efimov, *Sov. J. Nucl. Phys.* **29**, 546 (1979).
- [56] E. Alt, P. Grassberger, and W. Sandhas, *Nucl. Phys. B* **2**, 167 (1967), ISSN 0550-3213.
- [57] E. W. Schmid and H. Ziegelmann, *The quantum mechanical three-body problem* (Pergamon Press, Oxford, 1974).
- [58] P. M. A. Mestrom, T. Secker, R. M. Kroeze, and S. J. J. M. F. Kokkelmans, *Phys. Rev. A* **99**, 012702 (2019).
- [59] See Supplemental Material.
- [60] S. Weinberg, *Phys. Rev.* **131**, 440 (1963).
- [61] J. Wang, J. P. D’Incao, Y. Wang, and C. H. Greene, *Phys. Rev. A* **86**, 062511 (2012).
- [62] E. Braaten and H.-W. Hammer, *Phys. Rev. A* **70**, 042706 (2004).
- [63] D. S. Petrov, Three-boson problem near a narrow Feshbach resonance, Workshop on Strongly Interacting Quantum Gases (Ohio State University) (2005).
- [64] J. H. Macek, S. Yu Ovchinnikov, and G. Gasaneo, *Phys. Rev. A* **73**, 032704 (2006).
- [65] A. O. Gogolin, C. Mora, and R. Egger, *Physical Review Letters* **100**, 140404 (2008).
- [66] J. R. Taylor, *Scattering theory: The quantum theory on nonrelativistic collisions* (Wiley, 1972).

Supplemental Materials: “Elastic scattering of three ultracold bosons”

P. M. A. Mestrom,¹ V. E. Colussi,¹ T. Secker,¹ and S. J. J. M. F. Kokkelmans¹

¹*Eindhoven University of Technology, P. O. Box 513, 5600 MB Eindhoven, The Netherlands*

I. THE THREE-BODY SCATTERING HYPERVOLUME

Here we relate the three-body scattering hypervolume D to the transition amplitude $\langle \mathbf{p}, \mathbf{q} | U_{00}(0) | \mathbf{0}, \mathbf{0} \rangle$ for identical bosons interacting via pairwise local symmetric potentials. Tan [18] defined the three-body scattering hypervolume D via the zero-energy three-body scattering wave function $|\Psi_{3b}(0)\rangle = |\mathbf{0}, \mathbf{0}\rangle + G_0(0)U_{00}(0)|\mathbf{0}, \mathbf{0}\rangle$, whose momentum-space representation is given by

$$\begin{aligned} \langle \mathbf{p}, \mathbf{q} | \Psi_{3b}(0) \rangle &= \langle \mathbf{p} | \mathbf{0} \rangle \langle \mathbf{q} | \mathbf{0} \rangle \\ &- \frac{1}{\frac{p^2}{m} + \frac{3q^2}{4m}} \langle \mathbf{p}, \mathbf{q} | U_{00}(0) | \mathbf{0}, \mathbf{0} \rangle. \end{aligned} \quad (\text{S1})$$

In order to determine the behavior of the matrix element $\langle \mathbf{p}, \mathbf{q} | U_{00}(0) | \mathbf{0}, \mathbf{0} \rangle$, we analyze the AGS equations for identical bosons. As presented in Ref. [58], we define the operator $\check{U}_{\alpha 0}(z) \equiv T_{\alpha}(z)G_0(z)U_{\alpha 0}(z)(1+P)$ where P is the sum of the cyclic and anticyclic permutation operators. It satisfies the inhomogeneous equation [58]

$$\check{U}_{\alpha 0}(z) = T_{\alpha}(z)(1+P) + T_{\alpha}(z)G_0(z)P\check{U}_{\alpha 0}(z). \quad (\text{S2})$$

From Eq. (2) of the main text, we derive that

$$U_{00}(z)(1+P) = \sum_{\alpha=1}^3 \check{U}_{\alpha 0}(z), \quad (\text{S3})$$

which gives

$$\langle \mathbf{p}, \mathbf{q} | U_{00}(z) | \mathbf{0}, \mathbf{0} \rangle = \frac{1}{3} \sum_{\alpha=1}^3 \alpha \langle \mathbf{p}_{\alpha}, \mathbf{q}_{\alpha} | \check{U}_{\alpha 0}(z) | \mathbf{0}, \mathbf{0} \rangle. \quad (\text{S4})$$

The index α in $|\mathbf{p}_{\alpha}, \mathbf{q}_{\alpha}\rangle_{\alpha}$ indicates that \mathbf{p}_{α} represents the relative momentum between particles β and γ , whereas \mathbf{q}_{α} represents the relative momentum between particle α and the center of mass of the two-particle system ($\beta\gamma$).

The singular behavior of $\alpha \langle \mathbf{p}_{\alpha}, \mathbf{q}_{\alpha} | \check{U}_{\alpha 0}(0) | \mathbf{0}, \mathbf{0} \rangle$ at $q_{\alpha} = 0$ can be determined by writing the operator $\check{U}_{\alpha 0}$ as a series and analyzing each term. We write Eq. (S2) as

$$\begin{aligned} \check{U}_{\alpha 0} &= T_{\alpha}(1+P) + T_{\alpha}G_0PT_{\alpha}(1+P) \\ &+ T_{\alpha}G_0PT_{\alpha}G_0PT_{\alpha}(1+P) + \dots \end{aligned} \quad (\text{S5})$$

where we removed the arguments of the operators for notational convenience. The first term on the right-hand-side represents two-particle scattering in which the third

particle only spectates,

$$\begin{aligned} \alpha \langle \mathbf{p}_{\alpha}, \mathbf{q}_{\alpha} | T_{\alpha}(0)(1+P) | \mathbf{0}, \mathbf{0} \rangle \\ = 3 \langle \mathbf{q}_{\alpha} | \mathbf{0} \rangle \langle \mathbf{p}_{\alpha} | T(0) | \mathbf{0} \rangle. \end{aligned} \quad (\text{S6})$$

The second term on the right-hand-side of Eq. (S5) behaves as

$$\begin{aligned} \alpha \langle \mathbf{p}_{\alpha}, \mathbf{q}_{\alpha} | T_{\alpha}(0)G_0(0)PT_{\alpha}(0)(1+P) | \mathbf{0}, \mathbf{0} \rangle \\ = -\frac{3}{2\pi^4} \frac{a^2}{m\hbar^2} \frac{1}{q_{\alpha}^2} - \frac{3\sqrt{3}}{4\pi^4} \frac{a^3}{m\hbar^3} \frac{1}{q_{\alpha}} \\ - 3m \langle \mathbf{0} | T(0) | \mathbf{0} \rangle \left[\left(\frac{5}{4} + \frac{p_{\alpha}^2}{q_{\alpha}^2} \right) \frac{\partial^2 \langle \mathbf{p} | T(0) | \mathbf{0} \rangle}{\partial p^2} \right]_{p=0} \\ + \left. \frac{\partial^2 \langle \mathbf{0} | T(-\frac{3}{4m}q^2) | \mathbf{0} \rangle}{\partial q^2} \right]_{q=0} + \mathcal{O}(q_{\alpha}, p_{\alpha}^4/q_{\alpha}^2). \end{aligned} \quad (\text{S7})$$

The small-momentum behavior of the third term is given by

$$\begin{aligned} \alpha \langle \mathbf{p}_{\alpha}, \mathbf{q}_{\alpha} | (T_{\alpha}(0)G_0(0)P)^2 T_{\alpha}(0)(1+P) | \mathbf{0}, \mathbf{0} \rangle \\ = \frac{1}{\pi^3} \frac{a^3}{m\hbar^3} \frac{1}{q_{\alpha}} - \frac{3\sqrt{3}}{\pi^5} \frac{a^4}{m\hbar^4} \ln \left(\frac{q_{\alpha}|a|}{\hbar} \right) \\ + \mathcal{O} \left(q_{\alpha}^0, \frac{p_{\alpha}^2}{q_{\alpha}} \right). \end{aligned} \quad (\text{S8})$$

It is a matter of choice to express the momentum q_{α} in units of $\hbar/|a|$ inside the logarithm. The next term in the expansion of $\alpha \langle \mathbf{p}_{\alpha}, \mathbf{q}_{\alpha} | \check{U}_{\alpha 0}(0) | \mathbf{0}, \mathbf{0} \rangle$ also diverges logarithmically in the limit $q_{\alpha} \rightarrow 0$:

$$\begin{aligned} \alpha \langle \mathbf{p}_{\alpha}, \mathbf{q}_{\alpha} | (T_{\alpha}(0)G_0(0)P)^3 T_{\alpha}(0)(1+P) | \mathbf{0}, \mathbf{0} \rangle \\ = \frac{4}{\pi^4} \frac{a^4}{m\hbar^4} \ln \left(\frac{q_{\alpha}|a|}{\hbar} \right) + \mathcal{O} \left(q_{\alpha}^0, p_{\alpha}^2 \ln(q_{\alpha}|a|/\hbar) \right). \end{aligned} \quad (\text{S9})$$

All other contributions to $\alpha \langle \mathbf{p}_{\alpha}, \mathbf{q}_{\alpha} | \check{U}_{\alpha 0}(0) | \mathbf{0}, \mathbf{0} \rangle$ are non-singular in $q_{\alpha} = 0$. From the above analysis we find that $\langle \mathbf{p}, \mathbf{q} | \Psi_{3b}(0) \rangle$ defined by Eq. (S1) can be written as

$$\begin{aligned}
\langle \mathbf{p}, \mathbf{q} | \Psi_{3b}(0) \rangle &= \delta(\mathbf{p})\delta(\mathbf{q}) - \frac{1}{\frac{p^2}{m} + \frac{3q^2}{4m}} \sum_{\alpha=1}^3 \left\{ \delta(\mathbf{q}_\alpha) \langle \mathbf{p}_\alpha | T(0) | \mathbf{0} \rangle - \frac{1}{2\pi^4} \frac{a^2}{m\hbar^2} \frac{1}{q_\alpha^2} + \frac{1}{12\pi^4} (4\pi - 3\sqrt{3}) \frac{a^3}{m\hbar^3} \frac{1}{q_\alpha} \right. \\
&+ \frac{1}{3\pi^5} (4\pi - 3\sqrt{3}) \frac{a^4}{m\hbar^4} \ln\left(\frac{q_\alpha |a|}{\hbar}\right) - \frac{p_\alpha^2 + \frac{3}{4}q_\alpha^2}{q_\alpha^2} m \langle \mathbf{0} | T(0) | \mathbf{0} \rangle \left. \frac{\partial^2 \langle \mathbf{p} | T(0) | \mathbf{0} \rangle}{\partial p^2} \right|_{p=0} + \frac{1}{3} \frac{1}{(2\pi)^6} \frac{D}{m\hbar^4} \quad (\text{S10}) \\
&+ \mathcal{O}\left(q_\alpha \ln\left(\frac{q_\alpha |a|}{\hbar}\right), \frac{p_\alpha^2}{q_\alpha}\right),
\end{aligned}$$

where we used the exactly same definition for D as the one presented by Tan [18]. The relation between D and $\langle \mathbf{p}, \mathbf{q} | U_{00}(z) | \mathbf{0}, \mathbf{0} \rangle$ is given in Eq. (3) of the main text.

II. HYPERVOLUME FOR WEAK INTERACTION STRENGTHS

In this section we analyze the behavior of the three-body scattering hypervolume corresponding to three identical bosons interacting via a symmetric pairwise potential $V(r) = v_0 f(r)$ in the limit $v_0 \rightarrow 0$. Here $f(r)$ is some function independent of v_0 that goes to zero sufficiently fast for increasing interparticle separation such that regular scattering theory is valid [66].

In the limit $v_0 \rightarrow 0$, we can approximate the two-body transition operator by the Born approximation $T(z) = V + \mathcal{O}(v_0^2)$. To determine the hypervolume D to the lowest order in v_0 , we consider the operator $T_\alpha(0)G_0(0)PT_\alpha(0)(1+P)$. Applying the Born approximation to Eq. (S7), we find

$$\begin{aligned}
&\alpha \langle \mathbf{0}, \mathbf{q}_\alpha | T_\alpha(0)G_0(0)PT_\alpha(0)(1+P) | \mathbf{0}, \mathbf{0} \rangle \\
&= -\frac{3}{2\pi^4} \frac{a^2}{m\hbar^2} \frac{1}{q_\alpha^2} - \frac{3\sqrt{3}}{4\pi^4} \frac{a^3}{m\hbar^3} \frac{1}{q_\alpha} \quad (\text{S11}) \\
&- \frac{15m}{4} \langle \mathbf{0} | V | \mathbf{0} \rangle \left. \frac{\partial^2 \langle \mathbf{q} | V | \mathbf{0} \rangle}{\partial q^2} \right|_{q=0} + \mathcal{O}(q_\alpha, v_0^3).
\end{aligned}$$

Comparing this result with Eq. (3) of the main text and using Eqs. (S4) and (S5), we find that

$$D = -96\pi^6 m^2 \hbar^4 \langle \mathbf{0} | V | \mathbf{0} \rangle \left. \frac{\partial^2 \langle \mathbf{p} | V | \mathbf{0} \rangle}{\partial p^2} \right|_{p=0} + \mathcal{O}(v_0^3) \quad (\text{S12})$$

as stated in the main text.

III. COMPARISON WITH BRAATEN ET AL. [51]

Braaten et al. [51] have calculated a three-body elastic scattering amplitude that is closely related to the amplitude $\langle \mathbf{0}, \mathbf{q} | U_{00}(0) | \mathbf{0}, \mathbf{0} \rangle$ that we calculate. The main

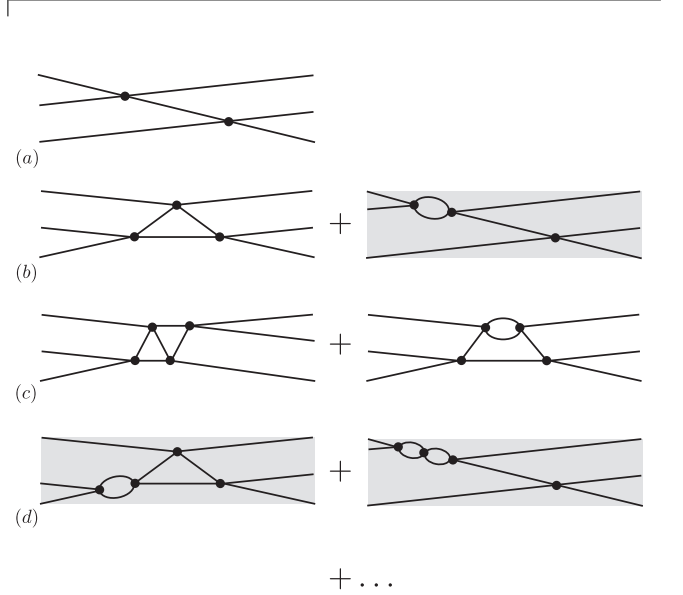


Figure S1: Feynman diagrams contributing to the q_α^{-2} behavior (a), the q_α^{-1} behavior (b), the $\ln(q_\alpha |a|/\hbar)$ behavior (c) and the nondiverging part (d) of the three-body elastic scattering amplitude $\langle \mathbf{p}, \mathbf{q} | U_{00}(0) | \mathbf{0}, \mathbf{0} \rangle$. The shaded diagrams are not included in the operator \mathcal{T} of Ref. [51]. The vertices represent the two-body interaction.

difference is that the three-body operator T as defined in Ref. [51] (which we denote by \mathcal{T} in the following as we already reserved T for the two-body transition operator) includes less scattering events than the AGS operator U_{00} . First of all, scattering processes in which the third particle spectates are not included in \mathcal{T} . Secondly, two-body scattering events that occur before the third particle participates in the scattering process are incorporated in so-called dimer propagators [4, 51] and are thus not included in \mathcal{T} . The same applies to two-body scattering events that occur after the third particle has moved away from the two-particle subsystem. For clarity, we show some Feynman diagrams for three-body elastic scattering in Fig. S1. This figure indicates which scattering events are not included in \mathcal{T} .

Consequently, some terms on the right-hand-side of Eq. (S7) are not included in the calculation of

$\langle \mathbf{0}, \mathbf{q} | \mathcal{T}(0) | \mathbf{0}, \mathbf{0} \rangle$, namely $-3\sqrt{3}/(4\pi^4)a^3/(m\hbar^3q_\alpha)$ and

$$\begin{aligned} & -3m\langle \mathbf{0} | T(0) | \mathbf{0} \rangle \frac{\partial^2 \langle \mathbf{0} | T(-\frac{3}{4m}q^2) | \mathbf{0} \rangle}{\partial q^2} \Big|_{q=0} \quad (\text{S13}) \\ & = -\frac{9}{8\pi^4} \frac{a^4}{m\hbar^4} + \mathcal{O}(a^3) \end{aligned}$$

where terms that grow less fast than a^4 are indicated by $\mathcal{O}(a^3)$. A similar analysis reveals that the right-hand-side of Eq. (S8) includes the term $\sqrt{3}/(2\pi^3)a^4/(m\hbar^4)$ which is absent in $\langle \mathbf{0}, \mathbf{q} | \mathcal{T}(0) | \mathbf{0}, \mathbf{0} \rangle$. All other scattering events that are incorporated in $\langle \mathbf{0}, \mathbf{q} | U_{00}(0) | \mathbf{0}, \mathbf{0} \rangle$, but not in $\langle \mathbf{0}, \mathbf{q} | \mathcal{T}(0) | \mathbf{0}, \mathbf{0} \rangle$ vanish in the limit $q \rightarrow 0$ or grow less fast than a^4 . So from this analysis combined with Eq. (3) of the main text, the connection between the hypervolume D and the quantity $A(a\Lambda_*)$ as defined by Ref. [51] can be made resulting in

$$\frac{1}{C} \left[\frac{1}{a^4} D - (2\pi)^6 \left(\frac{\sqrt{3}}{2\pi^3} - \frac{9}{8\pi^4} \right) \right] \Big|_{|a| \rightarrow \infty} \equiv A(a\Lambda_*). \quad (\text{S14})$$

The three-body parameter Λ_* depends on the considered two-body potential and is related to a_- and a_+ [4].

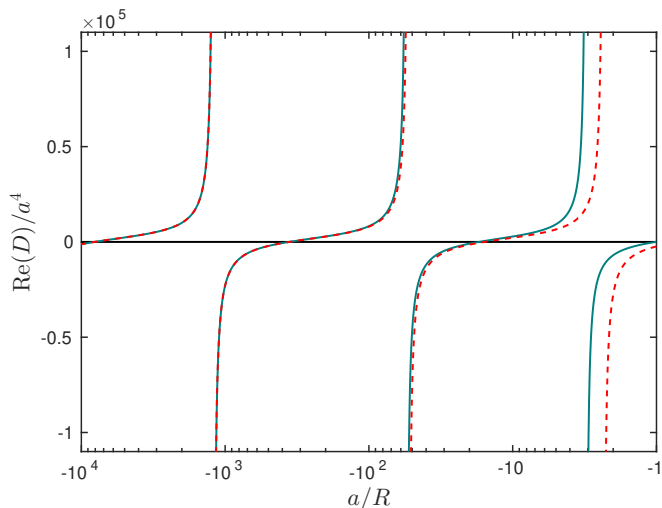


Figure S2: Three-body scattering hypervolume D near the first potential resonance of the square-well potential for $a < 0$. The dashed curve gives the analytic zero-range results given by Eq. (7) of the main text where we set $a_-/R = -1205$, $b_- = 3.153$, $c_- = 1.140$ and $\eta = 0$.

IV. CALCULATION OF THE THREE-BODY ELASTIC SCATTERING AMPLITUDE

Here we comment on the approach that we use to calculate the three-body elastic scattering amplitude $\langle \mathbf{0}, \mathbf{q} | U_{00}(0) | \mathbf{0}, \mathbf{0} \rangle$. In fact, we use the same method as presented in Ref. [58] to solve Eq. (S2) for the matrix elements $\alpha \langle \mathbf{0}, \mathbf{q} | \check{U}_{\alpha 0}(0) | \mathbf{0}, \mathbf{0} \rangle$ from which the elastic scattering amplitude is determined via Eq. (S4). So we

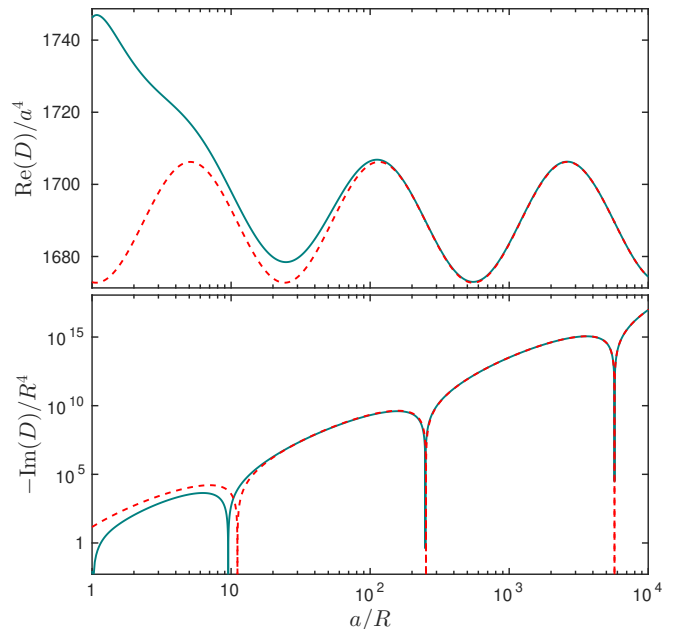


Figure S3: Three-body scattering hypervolume D near the first potential resonance of the square-well potential for $a > 0$. The dashed curves give the analytic zero-range results given by Eq. (8) and (10) of the main text where we set $a_+/R = 5720$, $b_+ = 0.0226$, $c_+ = 1.1288$, $C_+ = 67.118$ and $\eta = 0$.

write down the integral equations for the matrix elements $\alpha \langle \mathbf{0}, \mathbf{q} | \check{U}_{\alpha 0}(0) | \mathbf{0}, \mathbf{0} \rangle$, and expand them in partial waves and in form factors that are determined by the Weinberg expansion [58, 60]. The resulting integral equation is solved as a matrix equation by discretizing the magnitude of the momentum q . The amplitude $\alpha \langle \mathbf{0}, \mathbf{q} | \check{U}_{\alpha 0}(0) | \mathbf{0}, \mathbf{0} \rangle$ diverges as q^{-2} , q^{-1} and $\ln(q)$ in the limit $q \rightarrow 0$. We deal with these singularities by subtracting them from the matrix elements and solve the integral equations for the remaining part.

The number of partial-wave components that we need to take into account increases as the potential depth increases [58]. For three-body calculations near the first potential resonance of the square-well potential, it suffices to take $l = 0$ and $l = 2$, and to neglect the higher partial-wave components for a relative uncertainty of 10^{-3} . Near the second potential potential resonance, we take $l = 0, 2, 4, 6$ and 8 for the same precision, whereas for small scattering lengths in between the second and third potential resonance we also take $l = 10$ into account. The total number of Weinberg expansion terms that we take into account varies from 13 near the first potential resonance to 59 in between the second and third potential resonance.

Table S1: Values of characteristic parameters of the three-body scattering hypervolume D (real and imaginary part) corresponding to the N th potential resonance of the square-well potential. The three-body parameters $a_{-,n}$ and $a_{+,n}$ locate the trimer resonances corresponding to the $(n+1)$ th Efimov state. They are obtained by fitting the data close to the resonance position with Eq. (7) of the main text for $a_{-,n}$ and Eq. (10) of the main text for $a_{+,n}$. We only consider the three-body parameters for $|a|/R < 10^4$. Consequently, we have not determined $a_{+,3}$ for $N = 2$. The loss parameter η is determined by fitting the numerical data in the strongly-interacting regime ($10^3 < |a|/R < 10^4$).

N	$a_{-,0}/R$	$a_{-,1}/R$	$a_{-,2}/R$	$a_{+,0}/R$	$a_{+,1}/R$	$a_{+,2}/R$	$a_{+,3}/R$	η
1	-3.087(1)	-54.90(1)	-1205(1)	1.015(1)	9.530(1)	249.7(1)	5720(1)	0
2	-17.43(1)	-372.1(1)	-8396(1)	1.21(5)	75.7(1)	1759(5)	-	0.068(1)

V. ADDITIONAL RESULTS FOR THE FIRST AND SECOND POTENTIAL RESONANCE

We have also calculated the three-body scattering hypervolume D in the strongly-interacting regime near the first potential resonance corresponding to the square-well interaction. These results are presented in Fig. S2 for $a < 0$ and in Fig. S3 for $a > 0$, in which they are compared to the analytic zero-range results. An overview of the three-body parameters a_- and a_+ is given in Table S1. Our result for the loss parameter η in Table S1 is the same for large positive and negative scattering lengths near the second potential resonance and is consistent with the results of Ref. [58] from which it can be inferred that η is expected to be in between 0.06 and 0.08 for $|a|/R \gg 1$.

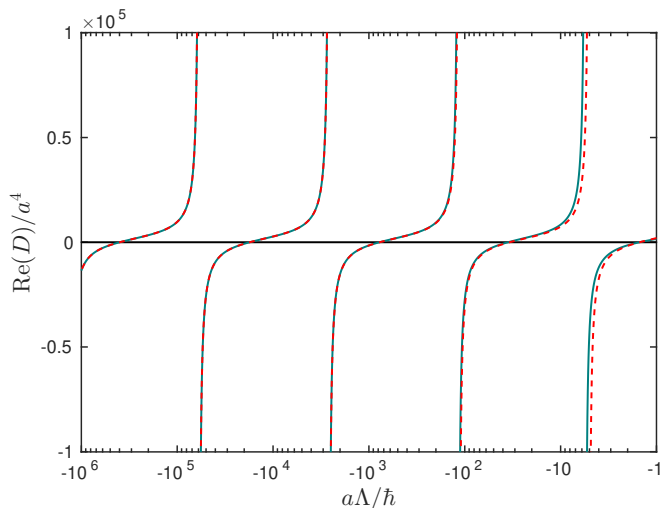


Figure S4: Three-body scattering hypervolume D near the potential resonance of the contact interaction with momentum cut-off Λ for $a < 0$. The dashed curve gives the analytic zero-range results given by Eq. (7) of the main text where we set $a_- \Lambda/\hbar = -5.926 \cdot 10^4$, $b_- = 3.153$, $c_- = 1.140$ and $\eta = 0$.

VI. UNIVERSAL PARAMETERS

The universal coefficients appearing in the analytic zero-range results (see Eq. (7)–(10) in the main text) can be most easily determined from the contact interaction itself. Since we work in momentum space, we add a momentum cut-off Λ to the contact interaction, i.e.,

$$V = -\zeta|g\rangle\langle g|, \quad (\text{S15})$$

where

$$\langle \mathbf{p}|g\rangle = \begin{cases} 1, & 0 \leq p \leq \Lambda, \\ 0, & p > \Lambda. \end{cases} \quad (\text{S16})$$

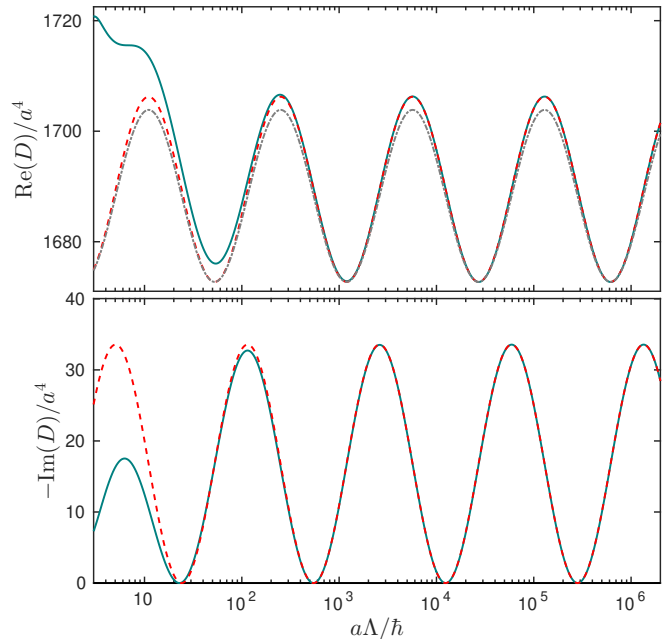


Figure S5: Three-body scattering hypervolume D near the potential resonance of the contact interaction with momentum cut-off Λ for $a > 0$. The red dashed curves give the analytic zero-range results given by Eq. (8) and (10) of the main text where we set $a_+ \Lambda/\hbar = 2.82 \cdot 10^5$, $b_+ = 0.0226$, $c_+ = 1.1288$, $C_+ = 67.118$ and $\eta = 0$. The gray dash-dotted curve displays the analytic zero-range result given by Eq. (8) of the main text with the same parameters except for $b_+ = 0.021$ which is the value reported in Ref. [51].

The scattering length can be changed by tuning the interaction strength ζ . The three-body scattering hypervolume D is calculated according to the same procedure as presented in the main text. Since the contact interaction is separable, there is only one potential resonance and the loss parameter η that appears in the universal equations (see Eq. (7)–(10) in the main text) is zero.

Our results for the contact interaction with a momentum cut-off are shown in Fig. S4 for $a < 0$ and in Fig. S5 for $a > 0$. We determine the universal coefficients C_+ , b_{\pm} and c_{\pm} from the characteristic points of these curves. First of all, the coefficient C_+ can be determined from the local maxima of $-\text{Im}(D/a^4)$ as presented in Table S2. Our results show that $C_{+,n}$ converges to $C_+ = 67.118(5)$ for $a \rightarrow \infty$.

Similarly, b_+ and c_+ can be determined from the local maxima and minima of $\text{Re}(D/a^4)$. The results of our analysis can be found in Table S3 from which we conclude that $b_+ = 0.0226(5)$ and $c_+ = 1.1288(5)$.

For negative scattering lengths, D is real and diverges at scattering lengths equal to the three-body parameters $a_{-,n}$. The behavior of D is given by Eq. (7) of the main text. By multiplying $D/(Ca^4)$ with $\sin(s_0 \ln(a/a_{-,n}))$, we remove the singularity in D at $a = a_{-,n}$. The resulting quantity behaves at scattering lengths near $a_{-,n}$ as

$$\frac{D/(Ca^4) \sin(s_0 \ln(a/a_{-,n}))}{\cos(s_0 \ln(a/a_{-,n}) - \delta_{-,n})} = \sqrt{b_{-,n}^2 + c_{-,n}^2} \quad (\text{S17})$$

where

$$\cos(\delta_{-,n}) = \frac{b_{-,n}}{\sqrt{b_{-,n}^2 + c_{-,n}^2}} \quad (\text{S18})$$

or

$$\sin(\delta_{-,n}) = \frac{c_{-,n}}{\sqrt{b_{-,n}^2 + c_{-,n}^2}}. \quad (\text{S19})$$

We determine the amplitude $\sqrt{b_{-,n}^2 + c_{-,n}^2}$ and phase shift $\delta_{-,n}$ from our numerical data of D . The resulting values of $b_{-,n}$ and $c_{-,n}$ can be found in Table S4.

The coefficients $c_{-,n}$ converge faster than $b_{-,n}$ and we conclude that $b_- = 3.153(5)$ and $c_+ = 1.140(2)$.

Table S2: Parameters corresponding to the local maxima of $-2 \cdot \text{Im}(D/a^4)$ calculated for the potential given by Eq. (S15). The local maxima are indicated by $C_{+,n}$ and the scattering lengths at which these maxima occur are indicated by $a_{\text{Im},n}$.

n	$a_{\text{Im},n}\Lambda/\hbar$	$C_{+,n}$
2	$1.145(5) \cdot 10^2$	65.453(5)
3	$2.61(1) \cdot 10^3$	67.045(5)
4	$5.93(1) \cdot 10^4$	67.114(5)
5	$1.344(3) \cdot 10^6$	67.118(5)

Table S3: Parameters corresponding to the local maxima and minima of $\text{Re}(D/a^4)/C$ calculated for the potential given by Eq. (S15). The local minima are indicated by $c_{+,n}$ and are located at $a = a_{\text{min},n}$, whereas $b_{+,n}$ is determined from the difference between the local maximum at $a = a_{\text{max},n}$ and minimum at $a = a_{\text{min},n}$.

n	$a_{\text{max},n}\Lambda/\hbar$	$a_{\text{min},n}\Lambda/\hbar$	$b_{+,n}$	$c_{+,n}$
1	-	$5.39(2) \cdot 10^1$	-	1.1310(5)
2	$2.47(1) \cdot 10^2$	$1.198(5) \cdot 10^3$	0.02277(50)	1.1289(5)
3	$5.68(3) \cdot 10^3$	$2.72(1) \cdot 10^4$	0.02265(50)	1.1288(5)
4	$1.29(3) \cdot 10^5$	$6.17(5) \cdot 10^5$	0.02265(50)	1.1288(5)

Table S4: Values of $b_{-,n}$ and $c_{-,n}$ that are determined from the amplitude and phase shift of the oscillatory function $D/(Ca^4) \sin(s_0 \ln(a/a_{-,n}))$ for the potential given by Eq. (S15). The amplitude $\sqrt{b_{-,n}^2 + c_{-,n}^2}$ and phase shift $\delta_{-,n}$ are determined near the $(n+1)$ th Efimov resonance that occurs at $a = a_{-,n}$.

n	$a_{-,n}\Lambda/\hbar$	$\delta_{-,n}$	$\sqrt{b_{-,n}^2 + c_{-,n}^2}$	$b_{-,n}$	$c_{-,n}$
1	$-1.169(1) \cdot 10^2$	0.3491(10)	3.3175(5)	3.117(2)	1.135(3)
2	$-2.614(1) \cdot 10^3$	0.3473(10)	3.3497(5)	3.150(2)	1.140(3)
3	$-5.926(1) \cdot 10^4$	0.3470(10)	3.3525(5)	3.153(2)	1.140(3)